Modeling Free Radical Ethylene Polymerization with Multifunctional Comonomers in Tubular Reactors: Influence on Microstructural LDPE Properties

Isabel Kadel,[1] *Thomas Herrmann,*[2] *Markus Busch**[1]

Summary: A kinetic model is developed to predict the effect of multi-functional comonomers in the high-pressure polymerization of ethylene in industrial tubular reactors. Two different modified acrylate based comonomers were tested in the simulation for their influence on molecular-weight distribution and branching densities. A comparison of both methods shows their potential to be used in an industrial process.

Keywords: crosslinking; gelation; kinetic modeling; LDPE; multifunctional comonomer; tubular reactor

Introduction

The high-pressure free radical polymerization of ethylene is a well-established industrial process for the production of low-density polyethylene (LDPE). Nevertheless the optimization and modification of LDPE for certain application properties is still of economic and scientific interest. At the moment the substitution of autoclave LDPE reactors for tubular LDPE reactors is an important goal for extrusion coating grades. The reasons for the efforts in this direction are the age, the smaller plant size and the higher energy consumption of autoclaves compared to existing tubular reactors.[1]

This project is quite challenging due to the fact that the microstructure of polyethylene and therefore its application properties strongly depend on the reactor type.[2] On that account the development of autoclave characteristics requires a special modification of typical tubular LDPE techniques. Because variation of process parameters like temperature and pressure is limited, the usage of certain comonomers is an appropriate tool to direct microstructural properties of polyethylene over a broad range. An adequate comonomer should lead to a broadening of the molecular-weight distribution (MWD) in the high-molecular-weight area and an increase in the long-chain branching density to reach the typical MWD of autoclaves in tubular reactors (Figure 1).

In principle there are two possible scenarios imaginable to generate autoclave-like structures via comonomer insertion. On the one hand it is possible to use bifunctional monomers (e.g. alkadienes, biacrylates) to generate long, crosslinked chains.[3,4] On the other hand one can introduce a comonomer with a chain transfer functionality (e.g. acrylate with aldehyde group), which allows the formation of additional long-chain branches in the growing polymer chain. Both methods have the potential to yield the desirable microstructural properties.

To estimate the effect of these agents before starting a novel process it is reasonable to check their performance on the polyethylene macromolecules using detailed kinetic modeling. With the help of the simulation program *Predici*[5] it is

[1] Technische Universität Darmstadt, Ernst-Berl-Institut, Petersenstr. 20, 64287 Darmstadt, Germany E-mail: busch@chemie.tu-darmstadt.de
[2] Basell Polyolefine GmbH, Industriepark Hoechst, Building: C 657, 65926 Frankfurt a. M., Germany

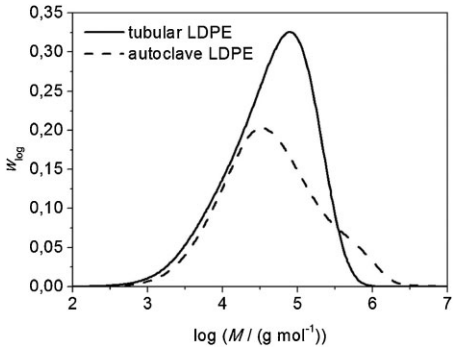

Figure 1.
Typical molecular-weight distributions of LDPE from industrial tubular reactors and continuous stirred autoclaves.

possible to develop a kinetic model for each copolymerization system in an industrial tubular reactor to describe the influence on important microstructural parameters.

Kinetic Model

The development of both kinetic models is based on the same standard free radical polymerization model for ethylene and an acrylate comonomer in an existing four-zone tubular reactor, which is geared to the Lupotech TS process from LyondellBasell.[6]

This basic model describes the full reaction network considering all possible homo- and crossreaction steps. Scheme 1 summarizes the implemented reaction equations.

Regarding the transfer to propionic aldehyde it has to be mentioned that due to lack of detailed information concerning the formed PA radicals, they are treated as primary ethylene radicals in the model.

For the kinetic description of this copolymerization the implicit penultimate model postulated by Fukuda[7–9] is used. With the aid of this technique the effect of the penultimate monomer unit on the rate constant of a growing macroradical is considered. For the calculation of the homo- and crosspropagation rate constants, the reactivity ratios r_1 and r_2 and the radical reactivity ratios s_1 and s_2 are needed.

$$r_1 = \frac{k_{p,11}}{k_{p,12}} \tag{1}$$

$$r_2 = \frac{k_{p,22}}{k_{p,21}} \tag{2}$$

$$s_1 = \frac{k_{p,211}}{k_{p,111}} \tag{3}$$

$$s_2 = \frac{k_{p,122}}{k_{p,222}} \tag{4}$$

and

$$s_1 = s_2 = \sqrt{r_1 r_2} \tag{5}$$

With these parameters the propagation rate constants can be calculated using the following relations:

$$k_{p,11} = k_{p,111}\frac{r_1 f_1 + f_2}{r_1 f_1 + \frac{f_2}{s_1}} \tag{6}$$

$$k_{p,22} = k_{p,222}\frac{r_2 f_2 + f_1}{r_2 f_2 + \frac{f_1}{s_2}} \tag{7}$$

$k_{p,iii}$ is the propagation rate constant for the homopolymerization of component i and f_i is the mol part of monomer i in the reaction mixture.

To describe termination kinetics according to Fukuda,[10] a composition dependent averaged rate constant k_t is implemented:

$$k_t = \left(\frac{F_1}{k_{t,1}} + \frac{F_2}{k_{t,2}}\right)^{-1} \tag{8}$$

$k_{t,i}$ is the termination rate constant for the homopolymerization of component i and F_i is the mol part of monomer i in the copolymer.

The corresponding kinetic rate coefficients for each homo- and crossreaction step in Scheme 1 are available in open literature.

For ethylene homopolymerization kinetics, the arrhenius data published by Busch were used.[11] The equations are listed in Table 1.

According to Schweer[12] the propagation and termination depends on the conversion of ethylene to polymer. To describe the diffusion limited rate constant, the known correlations from literature are used for the ethylene homopolymerization.

$I_2 \xrightarrow{k_{d,I}} 2R\text{-}I$	Initiator decomposition
$R\text{-}I + E \xrightarrow{\bar{k}_{p,11}\cdot f} R\text{-}E_1$	Initiation with E
$R\text{-}I + Ac \xrightarrow{\bar{k}_{p,22}\cdot f} R\text{-}Ac_1$	Initiation with Ac
$R\text{-}E_s + E \xrightarrow{\bar{k}_{p,11}} R\text{-}E_{s+1}$	Homopropagation of E
$R\text{-}E_s + Ac \xrightarrow{\bar{k}_{p,12}} R\text{-}Ac_{s+1}$	Crosspropagation to Ac
$R\text{-}Ac_s + E \xrightarrow{\bar{k}_{p,21}} R\text{-}E_{s+1}$	Crosspropagation to E
$R\text{-}Ac_s + Ac \xrightarrow{\bar{k}_{p,22}} R\text{-}Ac_{s+1}$	Homopropagation of Ac
$R\text{-}E_s + R\text{-}E_r \xrightarrow{\bar{k}_t} P_{s+r}$	Homotermination by combination of E
$R\text{-}E_s + R\text{-}Ac_r \xrightarrow{\bar{k}_t} P_{s+r}$	Crosstermination by combination
$R\text{-}Ac_s + R\text{-}Ac_r \xrightarrow{\bar{k}_t} P_{s+r}$	Homotermination by combination of Ac
$R\text{-}E_s + R\text{-}E_r \xrightarrow{\bar{k}_t} P_s + P_r$	Homotermination by disproportionation of E
$R\text{-}E_s + R\text{-}Ac_r \xrightarrow{\bar{k}_t} P_s + P_r$	Crosstermination by disproportionation
$R\text{-}Ac_s + R\text{-}Ac_r \xrightarrow{\bar{k}_t} P_s + P_r$	Homotermination by disproportionation of Ac
$R\text{-}E_s + E \xrightarrow{\bar{k}_{tr\text{-}m,11}} P_s + R\text{-}E_1$	Homotransfer to E
$R\text{-}E_s + Ac \xrightarrow{\bar{k}_{tr\text{-}m,12}} P_s + R\text{-}Ac_1$	Crosstransfer to Ac
$R\text{-}Ac_s + E \xrightarrow{\bar{k}_{tr\text{-}m,21}} P_s + R\text{-}E_1$	Crosstransfer to E
$R\text{-}Ac_s + Ac \xrightarrow{\bar{k}_{tr\text{-}m,22}} P_s + R\text{-}Ac_1$	Homotransfer to Ac
$R\text{-}E_s + PA \xrightarrow{\bar{k}_{tr\text{-}PA,1}} P_s + R\text{-}E_1$	Transfer of an E radical to PA
$R\text{-}Ac_s + PA \xrightarrow{\bar{k}_{tr\text{-}PA,2}} P_s + R\text{-}E_1$	Transfer of an Ac radical to PA
$R\text{-}E_s \xrightarrow{\bar{k}_{bb,11}\cdot F_1} R - E_{s,sec} + SCB$	Backbiting of an E radical to an E unit
$R\text{-}E_s \xrightarrow{\bar{k}_{bb,11}\cdot F_2\cdot Fac_{bb,I}} R\text{-}Ac_{s,sec} + SCB$	Backbiting of an E radical to an Ac unit
$R\text{-}Ac_s \xrightarrow{\bar{k}_{bb,22}\cdot F_1\cdot Fac_{bb,II}} R\text{-}E_{s,sec} + SCB$	Backbiting of an Ac radical to an E unit
$R\text{-}Ac_s \xrightarrow{\bar{k}_{bb,22}\cdot F_2} R\text{-}Ac_{s,sec} + SCB$	Backbiting of an Ac radical to an Ac unit
$R\text{-}E_s + P_r \xrightarrow{\bar{k}_{tr\text{-}pol,11}\cdot r\cdot F_1} P_s + R\text{-}E_{r,sec}$	Homotransfer to polymer
$R\text{-}E_s + P_r \xrightarrow{\bar{k}_{tr\text{-}pol,11}\cdot r\cdot F_2\cdot Fac_{tr\text{-}pol,I}} P_s + R\text{-}Ac_{r,sec}$	Crosstransfer to polymer
$R\text{-}Ac_s + P_r \xrightarrow{\bar{k}_{tr\text{-}pol,22}\cdot r\cdot F_1\cdot Fac_{tr\text{-}pol,II}} P_s + R\text{-}E_{r,sec}$	Crosstransfer to polymer

Scheme 1. (*continued*)

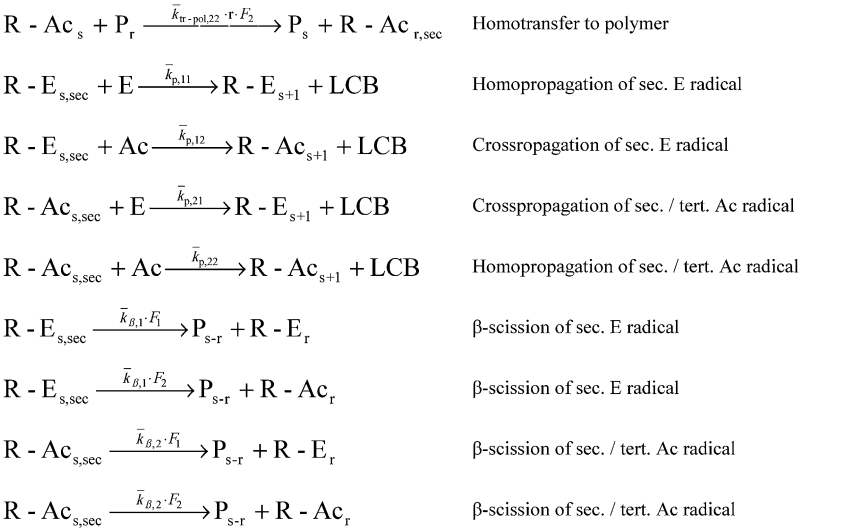

I :	Initiator	$k_{p,ij}$:	Rate constant for reaction x from species i-terminated radical to species j
E:	Ethylene		
Ac:	Acrylate	r, s :	Chain-length
R-I :	Initiator radical	f :	Initiator efficiency
R-E :	Ethylene radical	sec/tert:	Secondary/tertiary radical
R-Ac:	Acrylate radical	F_i:	Mol fraction of monomer i in copolymer
P:	Polymer	*Fac*:	Factors to describe cross reactions
SCB:	Short-chain branch	F_i:	Mol fraction of monomer i in copolymer
LCB:	Long-chain branch	*Fac*:	Factors to describe cross reactions

Scheme 1.
Full reaction network for ethylene acrylate copolymerization.

Table 1.
Rate coefficients according to ethylene homopolymerization steps shown in Scheme 1. p in bar, T in K, $R = 8.314\ \mathrm{J\,mol^{-1}\,K^{-1}}$.[11]

elementary reaction	arrhenius
Propagation[a] $[\mathrm{L \cdot mol^{-1} \cdot s^{-1}}]$	$k^0_{p,111} = 1.88{\cdot}10^7 \cdot e^{\left(-\frac{34300-2.7\cdot p}{R\cdot T}\right)}$
Termination[a] $[\mathrm{L \cdot mol^{-1} \cdot s^{-1}}]$	$k^0_{t,1} = 8.11{\cdot}10^8 \cdot e^{\left(-\frac{4600+1.58\cdot p}{R\cdot T}\right)}$
Transfer to monomer $[\mathrm{L \cdot mol^{-1} \cdot s^{-1}}]$	$k_{tr\text{-}m,11} = 3.42{\cdot}10^8 \cdot e^{\left(-\frac{75950-0.56\cdot p}{R\cdot T}\right)}$
Transfer to PA $[\mathrm{L \cdot mol^{-1} \cdot s^{-1}}]$	$k_{tr\text{-}PA,1} = 3.44{\cdot}10^6 \cdot e^{\left(-\frac{26800-1.49\cdot p}{R\cdot T}\right)}$
Backbiting $[\mathrm{s^{-1}}]$	$k_{bb,11} = 1.60{\cdot}10^8 \cdot e^{\left(-\frac{45783-2.32\cdot p}{R\cdot T}\right)}$
Transfer to polymer[a,b] $[\mathrm{L \cdot mol^{-1} \cdot s^{-1}}]$	$k^0_{tr\text{-}pol,11} = 1.377{\cdot}10^8 \cdot e^{\left(-\frac{49154-0.34\cdot p}{R\cdot T}\right)}$
β-scission $[\mathrm{s^{-1}}]$	$k_{\beta,11} = 3.21{\cdot}10^8 \cdot e^{\left(-\frac{42562-3.08\cdot p}{R\cdot T}\right)}$

[a] rate coefficients k_i^0 are without conversion dependence. [b] adapted pre-exponential factor due to conversion dependence of transfer to polymer. Standard literature value for $k_{0,tr\text{-}pol} = 1.02 \cdot 10^8$.

Herrmann[13] illustrated that transfer to polymer kinetics were influenced by the same conversion dependence than termination due to the fact that in both cases two macroradicals interact.

Table 2 shows the considered conversion viscosity relations for propagation, termination and transfer to polymer.

Due to the fact, that no data comonomers is available for the considered multi-

Table 2.
Conversion dependence for propagation, termination and transfer to polymer and relative viscosity.

conversion dependence of $k_{p,111}$ [L · mol^{-1} · s^{-1}]	$k_{p,111}(X,\eta_r) = \frac{k^0_{p,111}}{1+\frac{k^0_{p,111}}{1.13\cdot10^{10}}\eta_r}$
conversion dependence of $k_{t,1}$ [L · mol^{-1} · s^{-1}]	$k_{t,1}(X,\eta_r) = \left(0.832\cdot\frac{1}{\eta_r} + 8.04\cdot10^{-6}\cdot(1-X)\cdot k_{p,111}(X,\eta_r)\right)\cdot k^0_{t,1}$
conversion dependence of $k_{tr\text{-}pol,11}$ [L · mol^{-1} · s^{-1}]	$k_{tr\text{-}pol,11}(X,\eta_r) = \frac{k_t(X,\eta,T,p)}{k^0_t}\cdot k^0_{tr\text{-}pol,11}$
relative viscosity η_r [1 … ∞]	$\eta_r(X) = 10^{\left(5.39\cdot X + 3.7\cdot\sqrt{X}\right)}$

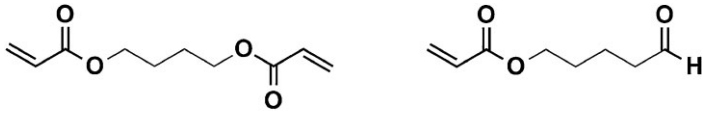

1 **2**

Figure 2.
Acrylic monomers for free radical copolymerization with ethylene; 1: Bifunctional acrylate (Ac-Ac); 2: Acrylate with chain-transfer functionality (Ac-CTA).

functional comonomers, reasonable assumptions for their homo- and copolymerization behavior have to be made. If the reactivity of the acrylate group is assumed to be independent from its rest, both copolymerizations could be described with the same rate coefficients concerning their acrylate functionalities. Because of the structural similarity to n-butyl acrylate (compare Figure 2), the homo- and copolymerization rate coefficients from this monomer were used preferentially. A detailed compilation of the implemented acrylate data is published by Becker.[14] In the following table the arrhenius expressions for acrylate homopolymerizations were listed.

It has to be noted that for transfer to propionic aldehyde equations from ethylene were used, because no information about the corresponding acrylate reaction is published.

To calculate the copolymerization of ethylene and (butyl-)acrylate several parameters are needed.

As shown in the Equation 1–7 the reactivity ratios are essential for the determination of all propagation reaction rates. For the developed model, we resort to data from Buback[15] for the ethylene n-

Table 3.
Rate constants k and transfer constants C according to acrylate homopolymerization steps shown in Scheme 1. p in bar, T in K, $R = 8.314$ J mol^{-1} K^{-1}. The index shows the belonging to a certain acrylate monomer.

elementary reaction	arrhenius
Propagation[a] [L · mol^{-1} · s^{-1}]	$k_{p,222} = 2.13\cdot10^7\cdot e^{\left(-\frac{17800-1.15p}{R\cdot T}\right)}$
Termination[a] [L · mol^{-1} · s^{-1}]	$k_{t,2} = 2.57\cdot10^8\cdot e^{\left(-\frac{4000+1.6\cdot p}{R\cdot T}\right)}$
Transfer to monomer[b]	$C_{tr\text{-}m,22} = 2.14\cdot10^4\cdot e^{\left(-\frac{49600-0.66\cdot p}{R\cdot T}\right)}$
Transfer to PA[d] [L · mol^{-1} · s^{-1}]	$k_{tr\text{-}PA,2} = 3.44\cdot10^6\cdot e^{\left(-\frac{26800-1.49\cdot p}{R\cdot T}\right)}$
Backbiting[a] [s^{-1}]	$k_{bb,22} = 3.5\cdot10^7\cdot e^{\left(-\frac{29300}{R\cdot T}\right)}$
Transfer to polymer[c] [L · mol^{-1} · s^{-1}]	$k_{tr\text{-}pol,22} = 3.20\cdot10^6\cdot e^{\left(-\frac{21500+5.0\cdot p}{R\cdot T}\right)}$
β-scission[c] [mol L^{-1}]	$C_{\beta,2} = 8.96\cdot10^{-2}\cdot e^{\left(\frac{7760}{R\cdot T}\right)}\cdot\frac{k_{\beta,11}}{k_{p,11}}$

[a] n-butyl acrylate [b] 2-ethylhexylacrylate [c] methylacrylate [d] ethylene

Table 4.
Reactivity ratios for ethylene n-butyl acrylate copolymerization. p in bar, T in K, $R = 8.314\ \mathrm{J\,mol^{-1}\,K^{-1}}$.[15]

reactivity ratios	arrhenius
$r_E = r_1$	$r_E = 9.2{\cdot}10^{-1}{\cdot}e^{\left(-\frac{1353\,8-8.2p}{R\cdot T}\right)}$
$r_{Ac} = r_2$	$r_{Ac} = 1.6{\cdot}10^{-2}{\cdot}e^{\left(\frac{22200}{R\cdot T}\right)}$

butyl acrylate copolymerization compiled in the table below.

Furthermore, the crossreaction steps for transfer to polymer and backbiting requires additional coefficients ascertained by van Boxtel[16] (see corresponding steps in Scheme 1).

It is assumed that the inter- and intramolecular transfer to polymer is accelerated by the same factor, as rate should be mainly influenced by the stability of generated secondary and tertiary radicals. Within this idea the following equalizations are valid.

$$Fac_{\mathrm{bb,I}} = Fac_{\mathrm{tr\text{-}pol,I}} \tag{9}$$

$$Fac_{\mathrm{bb,II}} = Fac_{\mathrm{tr\text{-}pol,II}} \tag{10}$$

Due to lack of ethylene located short-chain branches from acrylate terminated radicals in ^{13}C-NMR of ethylene methyl acrylate copolymers, a transfer from acrylate radicals to ethylene is excluded.[16] Therefore, $Fac_{\mathrm{bb,II}} = Fac_{\mathrm{tr\text{-}pol,II}} = 0$. Concerning the crosstransfer from ethylene radicals to polymeric acrylate functionalities the expression below was found.

$$Fac_{\mathrm{bb,I}} = Fac_{\mathrm{tr\text{-}pol,I}} = 1.6 \cdot 10^{3} \cdot e^{\left(-\frac{19300}{R\cdot T}\right)} \tag{11}$$

Finally, an empirical factor Fac_{M} for the crosstransfer to monomeric species is introduced. The following equation was found by van Boxtel to match experimental molecular-weight distribution.

$$Fac_{\mathrm{M}} = \frac{C_{\mathrm{tr\text{-}m,12}} \cdot r_1}{C_{\mathrm{tr\text{-}m,11}}} = \frac{C_{\mathrm{tr\text{-}m,21}} \cdot r_2}{C_{\mathrm{tr\text{-}m,22}}} = 5.2 \cdot 10^{-5} \cdot e^{\left(\frac{35600}{R\cdot T}\right)} \tag{12}$$

After the presentation of the full qualitative and quantitative basic copolymerization network, the characteristics of each multifunctional monomer can be discussed. In the following paragraphs the main deviations from the standard model and the most important assumptions will be presented.

First, the crosslinking copolymerization with Ac-Ac is in focus. The main difference compared to the basic model is related to the possibility of Ac-Ac to create a pendant acrylate function inside a macromolecular chain via incorporation of the comonomer. This pendant polymerizable functionality allows the formation of LCBs and crosslinks (CL) following the mechanism in Figure 3.

To approximate the rates for this crosslinking copolymerization regarding the full

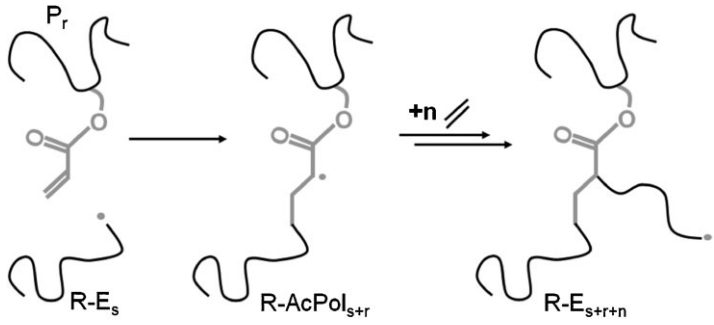

Figure 3.
Schematic reaction mechanism for crosslinking reaction. Example: Ethylene terminated radical R-E$_s$ reacts with the double bond of an acrylate function in a polymer P$_r$ under formation of a first LCB. The resulting secondary radical R-AcPol$_{s+r}$ interacts with monomer molecules and generates a CL between two polymer chains.

$$\mathrm{R\text{-}Ac_s + P_r \xrightarrow{\bar{k}_{p22}\cdot r\cdot F_{AcPol}\cdot Fac_{retard}} R\text{-}AcPol_{r+s,sec} + LCB}$$

$$\mathrm{R\text{-}E_s + P_r \xrightarrow{\bar{k}_{p12}\cdot r\cdot F_{AcPol}\cdot Fac_{retard}} R\text{-}AcPol_{r+s,sec} + LCB}$$

$$\mathrm{R\text{-}AcPol_s + E \xrightarrow{\bar{k}_{p,21}} R\text{-}E_{s+1} + CL}$$

$$\mathrm{R\text{-}AcPol_s + Ac\text{-}Ac \xrightarrow{\bar{k}_{p,22}} R\text{-}Ac_{s+1} + CL}$$

Scheme 2.
Reaction equations for modeling crosslinking reaction related to Figure 3. The first pair represents the crosslinking reactions and the second pair represents the formation of CLs as the consequential step. Assumptions 2–4 are taken into account.

reaction network, the assumptions below were stated.

1) Both acrylate functions in the monomer are treated independently as a single acrylate group. Therefore, rate coefficients listed above are used in general.
2) The reactivity of an acrylate double bond in polymer is 40% lower compared to the monomeric acrylate due to steric hindrance effects.[17] A retardation factor Fac_{retard} is introduced to reduce the propagation rates $k_{p,ij}$ in the crosslinking reaction (see Scheme 2).
3) The crosslinking reaction rate is weighted with the chain-length of the polymer containing a pendant double bond r and with the mol fraction of acrylate functions in this polymer F_{AcPol}. Consumption of pendant double bonds is included here.
4) The reactivity of the secondary radical formed by the propagation reaction at the pendant double bond (R-AcPol) equates to the reactivity of a normal acrylate terminated macroradical.
5) R-AcPol is considered to undergo each reaction listed in Scheme 1.
6) CLs are counted in the event of propagation and termination reactions where R-AcPol is involved.
7) Cyclization reactions are excluded from reaction network due to very low concentration of the comonomer in the feed.[18]

As the crosslinking reactions (see Figure 3) are the central steps in this model, the implemented reaction equations are shown in detail here.

All other reaction steps are implemented as shown in Scheme 1 regarding the assumptions above.

For the alternative approach using a chain transfer comonomer Ac-CTA the modification of the polymer architecture is related to the formation of additional long-chain branches due to introduction of a transfer functionality into a macromolecular species.

The corresponding reaction scheme is visualized in Figure 4.

In analogy to the first copolymerization system several assumptions have to be made to estimate reasonable rates for all possible reaction steps.

1) The acrylate and the transfer functionality are treated kinetically independent from each other. Acrylate kinetics from the basic model are used for acrylate functionality
2) Two different transfer reactions involving the comonomer are considered:
   - transfer to monomeric CTA group
   - transfer to pendant polymeric CTA group
3) The transfer group in the monomer and the polymer, represented by an aldehyde functionality, has the same rate constant as propionic aldehyde $k_{tr\text{-}PA}$. Under the assumption that the rate of the transfer is mainly influenced by the

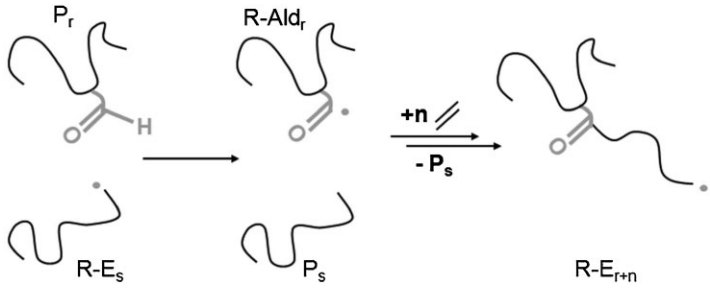

Figure 4.
Schematic reaction mechanism for polymeric transfer to CTA. Example: Ethylene terminated radical R-E_s abstracts an aldehyde hydrogen in polymer P_r. The resulting aldehyde radical R-Aldr adds further monomer molecules under generation of a LCB. In the model R-Ald is treated like R-E (see assumptions below).

binding energy of the aldehyde hydrogen, data from ethylene homopolymerizations are allowed to be used.

4) The transferring Ac-CTA monomer is treated as a simple ethylene radical R-E (Scheme 3). Thus, the terminal acrylate double bond in the growing macroradical is neglected. An incorporation of this terminal functionality would yield an additional LCB. As the simulation revealed that maximum 0.1 LCB per 1000 carbon atoms (LCB/1000C) more could be formed by this mechanism the disregard of terminal acrylate functions is feasible.
5) The rate for transfer to the pendant aldehyde functionality is weighted with the chain-length of the polymer r containing a chain modifying group and with the mol fraction of aldehyde functions this polymer F_{CTAPol}. Consumption of pendant aldehyde hydrogen is included here.
6) As each aldehyde radical R-Ald (monomeric and polymeric) behaves like a ethylene radical R-E, it is considered to undergo each reaction listed in Scheme 1.
7) Additional LCBs are counted in the event of transfer to the polymeric aldehyde functionality.

Because transfer reactions are the central steps in the copolymerization of ethylene with Ac-CTA, the implemented reaction equations for monomeric and polymeric hydrogen abstraction are listed with the corresponding rate coefficients.

$$\mathrm{R\text{-}E_s + Ac\text{-}CTA \xrightarrow{\bar{k}_{tr\text{-}PA,1}} R\text{-}E_{s+1}}$$

$$\mathrm{R\text{-}Ac_s + Ac\text{-}CTA \xrightarrow{\bar{k}_{tr\text{-}PA,2}} R\text{-}E_{s+1}}$$

$$\mathrm{R\text{-}E_s + P_r \xrightarrow{\bar{k}_{tr\text{-}PA,1}\cdot r\cdot F_{CTAPol}} R\text{-}E_{s+1} + LCB}$$

$$\mathrm{R\text{-}Ac_s + P_r \xrightarrow{\bar{k}_{tr\text{-}PA,2}\cdot r\cdot F_{CTAPol}} R\text{-}E_{s+1} + LCB}$$

Scheme 3.
Reaction equations for modeling the considered transfer reactions related to Figure 4. The first pair represents the transfer to monomeric Ac-CTA. The second pair represents the transfer to polymeric CTA. Assumptions 2–7 are taken into account.

Results and Discussion

The extended models were used to compare the efficiency of the comonomer functionalization in terms of their performance on broadening the MWD to match the autoclave distribution. Therefore, feed mixtures with increasing amount of the acrylate compounds were tested as input for the tubular reactor model. For both cases the comonomer is added together with ethylene in the beginning of the tubular reactor (first reaction zone).

The considered four-zone reactor system generates a typical saw tooth tempera-

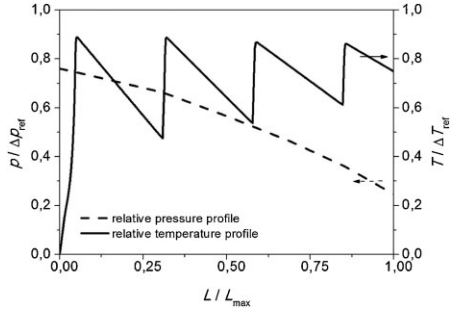

Figure 5.
Relative pressure and temperature profiles of the modelled industrial four-zone tubular reactor. The data is normalized with a reference value for pressure Δp_{ref} and temperature ΔT_{ref}.

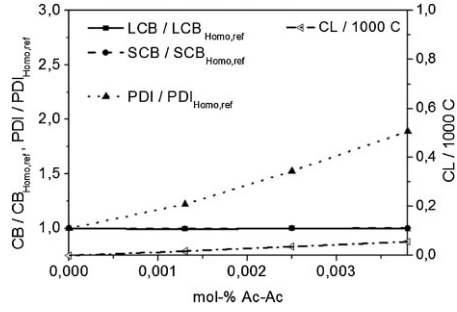

Figure 7.
Left axis: Influence of increasing amount of Ac-Ac comonomer on chain-branching (CB) including LCB and SCB and the polydispersity index (PDI). The data is normalized to the corresponding value from the homopolymerization. Right axis: Influence of increasing Ac-Ac comonomer amount on absolute CL/1000C.

ture profile and a typical pressure drop curve as illustrated in Figure 5.

Focusing on the bifunctional acrylate first, the simulated MWDs revealed that the addition of very small amounts of the comonomer - about 0.004 mol-% relative to the ethylene feed - causes a strong increase in the high-molecular-weight part of the distribution (Figure 6). The distribution becomes significantly broader and forms a hump in the high-molecular-weight region for higher comonomer contents.

As shown in Figure 7 a continuous increase in comonomer content leads to a continuous rise in polydispersity whereas the long- and short-chain branching densities are not affected by Ac-Ac addition. This behavior can be traced back to the formation of a very small amount of crosslinks per thousand carbon atoms (CL/1000C) being about two magnitudes lower than long-chain branches per thousand carbon atoms (LCB/1000C). Generally crosslinks show a very high sensitivity towards the polymer chain-length due to the fact that the connection of single macromolecules generates a three-dimensional network. Therefore, gelation is a current risk in this process. But with the help of the model it is possible to estimate limit concentrations for the comonomer in the feed to prevent gelation. The indicator for approaching the gel-point is the course of the weight-averaged molecular weight M_w: At the gel-point M_w runs to infinity and the simulation terminates at different positions inside the tubular reactor depending on the Ac-Ac concentration.

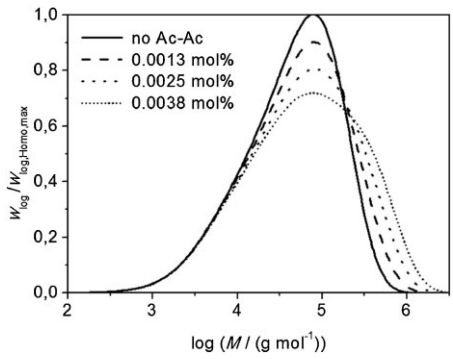

Figure 6.
Molecular-weight distribution of LDPE in dependence of Ac-Ac comonomer amount in the ethylene feed. The MWD is normalized to the maximum of the homo-polymer distribution.

Concerning the goal to reach autoclave-like MWD the crosslinking copolymerization shows the potential to form high-molecular-weight shoulders. A fine adjustment of the distinction of the shoulder could be realized later on by varying the reaction temperature.

For the second copolymerization system, where the chain-transfer acrylate Ac-CTA is used, the effect on microstructural

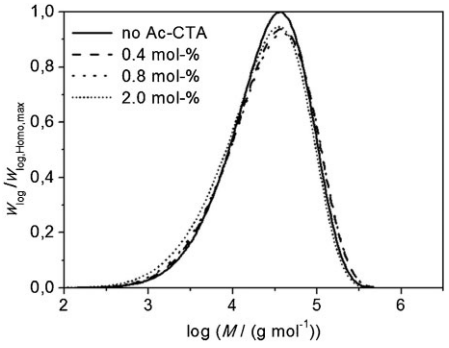

Figure 8.
Molecular-weight distribution of LDPE in dependence of Ac-CTA comonomer amount in the ethylene feed. The MWD is normalized to the maximum of the homo-polymer distribution.

parameters is completely different. As illustrated in Figure 8 the MWD shows an unexpected behavior: With increasing comonomer content the MWD broadens slightly in the high-molecular-weight area up to an amount of 0.8 mol-% in the feed mixture. Beyond this value the fraction of high-molecular-weight chains decreases in favor of the short-chain fraction.

This trend can also be relocated in the polydispersity curve in Figure 9. Nevertheless the number of LCBs increases nearly linearly with the Ac-CTA concentration, so that a continuous broadening of the distribution is expected. Inspecting the

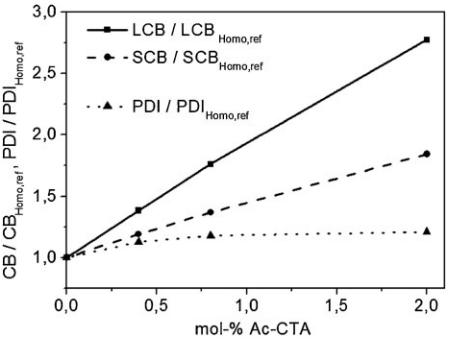

Figure 9.
Influence of increasing amount of Ac-CTA comonomer on chain-branching (CB) including LCB and SCB and the polydispersity index (PDI). The data is normalized to the corresponding value from the homopolymerization.

SCBs it is conspicuous, that the value increases with increasing amount of the acrylate in the feed mixture. This effect can be explained by the fact that ethylene terminated radicals show a strong backbiting on acrylate units in the same polymer chain (see acceleration factor $Fac_{bb,I}$ in Equation 11).

The reason for the untypical trend in the MWD and PDI can be ascribed to the chain-regulating effect of the aldehyde functionality in Ac-CTA. On the one hand the averaged chain-length of the polymer is reduced continuously with the Ac-CTA feed concentration, but on the other hand more and more LCBs are generated. If a certain comonomer content is exceeded the chain-shortening effect overcompensates the branching effect, so that the polydispersity shows a decreasing growth. With this self-regulating effect, gelation could be almost excluded in this copolymerization system. Therefore, the influence on the MWD is nearly negligible compared to the crosslinking polymerization system even though the comonomer contents are orders of magnitude higher. Finally, no real autoclave-like MWD can be reached with this method.

Conclusion

The simulation results revealed that the amount of injected comonomer plays a decisive role for the applicability of the particular process. Generally, crosslinking agents offer the possibility to develop a high-molecular-weight shoulder, as it is demanded for autoclave LDPE products. However, this approach includes the risk of gelation inside the tubular reactor depending on the monomer feed composition. Using chain-transfer comonomers leads to an inherently safe process with respect to gelation due to competitive effects of chain-shortening transfer reactions and formation of additional LCBs. But the typical MWD of autoclaves could not be achieved.

It could be shown that this simulation approach facilitates the comparison of

methods, shows limits and opportunities and enables the operator to find the most suitable process parameters.

[1] M. G. M. Neilen, J. J. J. Bosch, Proceedings of the 11th TAPPI European PLACE Conference **2007**, Athen.
[2] C. Kiparissides, J. F. MacGregor, G. Verros, *J. Macromol. Sci., Rev. Macromol. Chem. Phys.* **1993**, *33*, 437.
[3] P. Neuteboom, G. I. V. Bonte, J. C. J. F. Tacx, M. G. M. Neilen, US 2009/0234082, Sabic America, **2009**.
[4] P. Neuteboom, G. I. V. Bonte, J. C. J. F. Tacx, M. G. M. Neilen, WO 2006/094723, Sabic Polyethylenes B.V. **2006**.
[5] M. Wulkow, *Macromol. React. Eng.* **2008**, *2*, 461.
[6] C. Schmidt, M. Busch, D. Lillge, M. Wulkow, *Macromol. Mater. Eng.* **2005**, *290*, 404.
[7] T. Fukuda, Y. D. Ma, H. Inagaki, *Macromolecules* **1985**, *18*, 17–126.
[8] T. Fukuda, Y.-D. Ma, K. Kubo, A. Takada, *Polymer J.* **1989**, *21*, 1003–1009.
[9] T. Fukuda, Y.-D. Ma, H. Inagaki, *Makromol. Chem., Rapid Commun.* **1987**, *8*, 495–499.
[10] T. Fukuda, Y. D. Ma, K. Kubo, *Prog. Polym. Sci.* **1992**, *17*, 875–916.
[11] M. Busch, *Macromol. Theory Simul.* **2001**, *10*, 408–429.
[12] J. Schweer, *Ph.D. thesis*, Göttingen, **1988**.
[13] T. Herrmann, *Ph.D. thesis*, Darmstadt, **2011**.
[14] K. Becker, *PhD thesis*, Technische Universität Darmstadt, **2010**.
[15] M. Buback, T. Dröge, *Macromol. Chem. Phys.* **1997**, *198*, 3627–3638.
[16] H. C. M. van Boxtel, BT Ph.D. thesis, Göttingen, **2000**.
[17] D. T. Landin, C. W. Macosko, *Macromolecules* **1988**, *21*, 846–851.
[18] O. Okay, H. J. Nagash, *Macromol. Theory Simul.* **1995**, *4*, 967–981.

